SIAM J. Applied Dynamical Systems
Vol. 18, No. 4, pp. 1934–1953

Node-to-Node and Node-to-Medium Synchronization in Quorum Sensing Networks Affected by State-Dependent Noise*

Gaoyang Fan†, Giovanni Russo‡, and Paul C. Bressloff†

Abstract. A quorum sensing network is a form of communication system where nodes talk to each other through a shared environment or medium. Such networks arise in many applications, such as bacterial quorum sensing, where diffusing signaling molecules are exchanged with the extracellular environment, and in social networks, where decisions might be influenced by social media. In this paper, we analyze node-to-node and node-to-medium synchronization in these quorum sensing networks when nodes are affected by relative-state-dependent noise and the medium has a different dynamics from the nodes. By using stochastic Lyapunov arguments, we give a number of sufficient conditions for the stability of the synchronization manifold and compare the synchronization dynamics induced by common (extrinsic) noise and independent (intrinsic) noise. We also carry out a stochastic phase plane analysis of the dynamics on the synchronization manifold by introducing the notion of a stochastic invariant manifold.

Key words. quorum sensing networks, noise-induced synchronization, stochastic invariant manifold

AMS subject classifications. 93E03, 34D06, 60H10

DOI. 10.1137/19M1249515

1. Introduction.

Over the past few years, the study of noise-induced phenomena in complex networks of diffusively coupled dynamical systems (see, e.g., [6, 4, 21]) has attracted much attention. The study of collective opinion dynamics [1, 3], of coordination in biochemical systems [7], and of mean field dynamics [30] and memory effects in activity-driven networks [33] are just a few examples of applications where *noise* plays a key role in determining the global emerging behavior of the network (see also [27, 29]). Often, when studying noise-induced phenomena, it is assumed that nodes directly communicate with each other via exchanging information over a dedicated link. Unfortunately, this assumption is not satisfied for certain important applications. For example, in a biochemical context, it is often the case that network nodes (e.g., bacteria or neurons) communicate via a shared environmental medium [9, 20, 19, 14]. A classical example of these *quorum sensing* networks are bacteria, which communicate via signaling molecules (autoinducers) that diffuse in the extracellular environment so that cells can react as a group to different conditions [22, 24, 8, 12]. Another important example is opinion formation dynamics in networks under social media influence [32].

*Received by the editors March 12, 2019; accepted for publication (in revised form) by K. Josic August 23, 2019; published electronically November 7, 2019.
https://doi.org/10.1137/19M1249515

†Department of Mathematics, University of Utah, Salt Lake City, UT 84112 (gfan@math.utah.edu, bressloff@math.utah.edu).

‡School of Electrical and Electronic Engineering, University College Dublin, Dublin, 14, Ireland (giovanni.russo1@ucd.ie).

Often, when studying quorum sensing, the network dynamics is assumed to be noise-free, when in reality node-to-node or node-to-medium communication undergoes noise from different sources. Noise in network dynamics can generally be characterized as two types. Intrinsic noise is used to describe independent fluctuations caused by individual nodes or node-to-node links. On the other hand, extrinsic noise is used to represent common environmental noise that effects all nodes or node-to-node links in the network. A central question, which we address in this paper, is determining conditions under which node synchronization is achieved in the presence of either type of noise and how synchronization depends on the dynamics of the medium and the nature of the node-to-medium coupling. In particular, we consider the case where network nodes are affected by so-called relative-state-dependent (RSD) noise diffusion processes, which naturally arise in networks affected by quantization and/or fading communication channels (see, e.g., [31, 29]). Networks of N diffusively coupled nonlinear systems (without medium dynamics) affected by RSD noise diffusion process can be conveniently modeled (see [29] for the derivations) via the following stochastic differential equation (SDE):

$$dx_i = \left[f(x_i,t) + \sigma \sum_{j\in\mathcal{N}_i} C\cdot(x_j - x_i) \right] dt + \sigma^* \sum_{j\in\mathcal{N}_i} C\cdot g_{ij}(x_i - x_j, t)dW_{ij}, \quad i = 1,\dots,N, \tag{1.1}$$

where $x_i \in \mathbb{R}^n$, $f(x_i,t)$ denotes the internal node dynamics, $C \in \mathbb{R}^{n\times n}$ is a matrix specifying the coupling between internal degrees of freedom, σ is the coupling strength of the deterministic component of node-to-node links, and σ^* is the strength of the corresponding noisy component. Summation is over all nodes connected to node i, which are elements of the set $\mathcal{N}_i$. Finally, in (1.1), $g_{ij}(x_i - x_j, t)dW_{ij}$ represents the RSD noise diffusion process on the link (i,j) with W_{ij} denoting a Wiener process and with the functions $g_{ij}(\cdot,\cdot)$ being such that $g_{ij}(0,t) = 0\ \forall t$. Recently, in [29] it has been shown that, for network (1.1), synchronization can be induced by both extrinsic and intrinsic noise sources. This was done by studying the stability of the so-called synchronization manifold, i.e., the subset of $\mathbb{R}^n$ such that $x_1(t) = \cdots = x_N(t) = s(t)$.

In this context, after extending the SDE model developed in [29], we present a number of sufficient conditions for synchronization of quorum sensing networks affected by noise. In our model, nodes communicate indirectly via noisy node-to-medium links. In contrast to the SDE model in [29], our model allows the medium to undergo different internal dynamics from the nodes. Moreover, we formalize the notions of stochastic node-to-node and node-to-medium synchronization and analyze the stability of the corresponding synchronization manifolds. The proofs, which are obtained for both common and independent noise diffusion processes, leverage the use of stochastic Lyapunov functions [16]. Beyond the classical stability analysis, we also carry out a stochastic phase plane analysis of the dynamics on the synchronization manifold by introducing the notion of a stochastic invariant manifold, which allows us to study the path of convergence when synchronization conditions are satisfied.

The structure of this paper is as follows. In section 2, we set up the SDE that models the dynamics of a quorum sensing network with RSD noise. We then give a formal mathematical definition of synchronization and the various assumptions that are used in subsequent sections. In section 3, we analyze the synchronization condition under common noise and carry out a stochastic phase plane analysis. We illustrate our analysis using a model of opinion dynamics. In section 4, we extend the analysis to independent noise. Finally, in section 5, we summarize our results.

2. Problem setup. Before formally introducing the network dynamics considered in this paper, we give a number of results that will be used in our analysis.

2.1. Mathematical background. Consider an SDE (in the Itô sense) of the form [16, 23]

$$dx = a(x,t)dt + b(x,t)dW, \quad x_0 := x(t_0), \tag{2.1}$$

with $x \in \mathbb{R}^N$, $a : \mathbb{R}^N \times \mathbb{R}^+ \to \mathbb{R}^N$, and $b : \mathbb{R}^N \times \mathbb{R}^+ \to \mathbb{R}^{N\times N}$ and with W being an N-dimensional Wiener process. Also, assume that $a(0,t) = b(0,t) = 0\ \forall t$. We then have the following definition, where a.s. stands for "almost surely."

Definition 1. *The trivial solution $x(t) = 0$ of (2.1) is said to be a.s. exponentially stable if $\forall x_0 \in \mathbb{R}^N$, $\lim_{t\to+\infty} \sup \frac{1}{t} log(|x(t)|) < 0$, a.s.*

Let $V : \mathbb{R}^N \times \mathbb{R} \to \mathbb{R}$ be a smooth function and $V \in \mathscr{C}^{2,1}$, which means $V(x,t)$ is twice continuously differentiable in variable x and continuously differentiable in variable t. Let V_{xx} denote the Hessian matrix. Then, application of Itô's formula yields

$$dV(x,t) = LV(x,t)dt + V_x(x,t)b(x,t)dW, \tag{2.2}$$

where

1. $LV(x,t) = V_t(x,t) + V_x(x,t)a(x,t) + \frac{1}{2}tr\{b(x,t)^T V_{xx}(x,t)b(x,t)\}$;
2. $V_x = [V_{x_1}, \dots, V_{x_n}]$, where V_{x_i} represents the gradient with respect to x_i;
3. V_{xx} is the Hessian matrix with respect to x.

The following result from [16, Theorem 3.3, page 121] gives a sufficient condition for the trivial solution of to be a.s. exponentially stable.

Lemma 2.1. *Consider (2.1), and assume that there exists a nonnegative function $V(x,t) \in \mathscr{C}^{2\times1}$ and constants $p > 0, c_1 > 0, c_2 \in \mathbb{R}, c_2 \geq 0$ such that $\forall x \neq 0\ t \in \mathbb{R}^+$:*

(H1) $c_1|x|^p \leq V(x,t)$;
(H2) $LV(x,t) \leq c_2 V(x,t)$;
(H3) $|V_x(x,t)b(x,t)|^2 \geq c_3 V(x,t)^2$.

Then, $\lim_{t\to+\infty} \sup \frac{1}{t} log(|x(t)|) \leq -\frac{c_3-2c_2}{p}$, a.s. In particular, if $c_3 > 2c_2$, then the trivial solution of (2.1) is a.s. exponentially stable.

2.2. Network dynamics and synchronization. Consider a network consisting of N nodes labeled $i = 1, \dots, N$, which communicate indirectly via links to a shared medium. Let $x(t) \in \mathbb{R}^N$ and $z(t) \in \mathbb{R}$ denote the node and medium variables, respectively. Assume that the node-to-medium link is noisy and that the noise is RSD. Modifying the network model of [29], we have the following system of SDEs:

$$dx_i = [f(x_i,t) + \sigma(z - x_i)]dt + \widehat{\sigma}g(x_i - z)dW_i(t), \quad i = 1, \dots, N, \tag{2.3a}$$

$$dz = [h(z,t) - \sigma\sum_{j=1}^{N}(z - x_j)]dt - \widehat{\sigma}\sum_{j=1}^{N} g(x_j - z)dW_j(t), \tag{2.3b}$$

where $x_i(t) \in \mathbb{R}$, $f, h : \mathbb{R} \times \mathbb{R}_+ \to \mathbb{R}$ with f specifying the intrinsic node dynamics and h the intrinsic medium dynamics. The functions f and h model the dynamics that the nodes and

medium, respectively, would have if they were isolated, i.e., if there were no node-to-node or node-to-medium coupling. Moreover, $g : \mathbb{R} \to \mathbb{R}$ is a state-dependent noise diffusion process, and $W_j(t)$ is a Wiener process with noise intensity $\widehat{\sigma}$. If $W_j(t) = W(t)$ for all $j = 1, \ldots, N$, then we have common extrinsic noise, whereas if all the $W_j(t)$'s are independent, then we have independent intrinsic noise. We wish to remark here that the state-dependent noise diffusion processes considered in the paper naturally arise when modeling network systems where the communication undergoes quantization and/or when the channels experience fading [15, 31]. The functions f, g, h are taken to be smooth. Throughout the paper we will make the following assumptions.

Assumption 1. *There exists a constant K_f such that for all $x, y \in \mathbb{R}$ and $t > 0$, we have*

$$(x - y)[f(x, t) - f(y, t)] \leq K_f (x - y)^2. \tag{2.4}$$

The above condition is a global one-sided Lipschitz condition, also known as the QUAD condition [5]. Such a condition is satisfied by many chaotic systems such as the Lorentz system. Moreover, we assume the function g satisfies the following.

Assumption 2. *There exist constants $K_{g\pm}$, where $K_{g-} \leq K_{g+}$, such that for all $x, y \in \mathbb{R}$, we have*

$$K_{g-}|x - y| \leq |g(x) - g(y)| \leq K_{g+}|x - y|. \tag{2.5}$$

Here K_{g+} is the global Lipschitz constant for the function g, whereas K_{g-} provides a lower bound for $|g_x(x)|$. Such a lower bound exists for any function g since we can simply pick $K_{g-} = 0$. In our later analysis, we will discuss if there exist a strictly positive constant K_{g-} and how synchronization is affected by such a constant.

Let 1_N be the N-dimensional column vector of ones and $\otimes$ be the Kronecker (or direct) product. Then, throughout this paper, we assume that a solution of the form $\tilde{S}(t) := [S(t)^T, z(t)]^T$, with $S(t) := 1_N \otimes s(t)$, exists for (2.3). We term $\tilde{S}(t)$ as the synchronous solution of (2.3).

Essentially, in a quorum sensing network there are two *types* of synchronization phenomena: one where nodes synchronize regardless of the medium dynamics (node-to-node synchronization) and the other where all nodes and the medium are synchronized (node-to-medium synchronization). This leads to the following formal definition.

Definition 2. *Let $x_{i,0} := x_i(t_0)$, $i = 1, \ldots, N$ and $z_0 := z(t_0)$ be the initial conditions of the nodes and of the medium. System (2.3) achieves the following:*

1. **stochastic node-to-node synchronization** *if* $\forall x_{i,0} \in \mathbb{R}$,

$$\lim_{t \to +\infty} \sup \frac{1}{t} \log(|x_i(t) - s(t)|) < 0 \quad a.s. \quad \forall i = 1, \ldots, N. \tag{2.6}$$

2. **stochastic node-to-medium synchronization** *if, in addition, there exists some $\hat{s}(t)$ such that, for all initial conditions,*

$$\begin{aligned} &\lim_{t \to +\infty} \sup \frac{1}{t} \log(|z(t) - \hat{s}(t)|) < 0 \quad a.s. \\ &\lim_{t \to +\infty} \sup \frac{1}{t} \log(|s(t) - \hat{s}(t)|) < 0 \quad a.s. \end{aligned} \tag{2.7}$$

In the rest of the paper, we simply say that a network achieves node-to-node (node-to-medium) synchronization if Definition 2.1 (respectively, Definition 2.2) above is fulfilled. Note that, by definition, node-to-medium synchronization implies node-to-node synchronization, while the reverse is not true. Also, with Definition 2, we wish to point out that the node-to-node synchronous solutions $s(t)$ in Definition 2.1 and the node-to-medium synchronous solutions $\hat{s}(t)$ in Definition 2.2 can be, in general, different.

3. Network synchronization under common noise. We begin by considering the case where all node-to-medium connections in network (2.3) are subject to some common white noise, that is, $W_j(t) = W(t)$ for all $j = 1, \dots, N$. We can write down the corresponding SDE as

$$dx_i = [f(x_i, t) + \sigma(z - x_i)]dt + \widehat{\sigma} g(x_i - z)dW, \quad i = 1, \dots, N, \tag{3.1a}$$

$$dz = [h(z, t) - \sigma \sum_{j=1}^{N} (z - x_j)]dt - \widehat{\sigma} \sum_{j=1}^{N} g(x_j - z)dW. \tag{3.1b}$$

We first study node-to-node and node-to-medium synchronization using the classical a.s. stability approach of Mao [16]. We then study in more detail the stochastic dynamics on the synchronization manifold and demonstrate the presence of a stochastic trapping region, an invariant manifold, and bistability.

3.1. Node-to-node synchronization. First, we show that node-to-node synchronization can be achieved under common noise without having node-to-medium synchronization.

Theorem 3.1. *Consider* (3.1) *under Assumptions* 1 *and* 2. *The node dynamics,* $\mathbf{x}(t) = (x_1(t), \dots, x_N(t))$, *achieve node-to-node synchronization if the following condition holds:*

$$2\sigma > 2K_f + \widehat{\sigma}^2(K_{g+}^2 - 2K_{g-}^2). \tag{3.2}$$

Proof. To show that the nodes are synchronized, we write down the dynamics for the displacement between any two nodes and show that the relative displacement eventually goes to zero as $t \to \infty$. Without loss of generality, we study the relative displacements between nodes x_i with x_N for $i = 1, \dots, N-1$. That is, setting $e_i(t) = x_i(t) - x_N(t)$ we have

$$de_i = [f(x_N + e_i, t) - f(x_N, t) - \sigma e_i]dt + \widehat{\sigma}[g(x_N - z + e_i) - g(x_N - z)]dW.$$

Note that, for the above system, the dynamics of e_i and e_j are decoupled from each other for $i \neq j$ and $i, j \in \{1, \dots, N-1\}$. For notational simplicity, we can drop the index from the above equation so that

$$de = [f(x_N + e, t) - f(x_N, t) - \sigma e]dt + \widehat{\sigma}[g(x_N - z + e) - g(x_N - z)]dW.$$

It is clear that $e(t) \in \mathbb{R}$ and the trivial solution, $e = 0$, is an equilibrium solution. We want to show that the trivial solution is *a.s. exponentially stable*. Following Lemma 2.1 and setting $V(e, t) = \frac{1}{2}e^2$, we need to show that there exists constant $c_2 \in \mathbb{R}$, $c_3 \geq 0$ with $c_3 > 2c_2$

such that (H2) $LV(e,t) \le c_2 V(e,t)$ and (H3) $|V_e B|^2 \ge c_3 V^2$ for all (e, x_N, z). First, applying Assumptions 1 and 2, we have

$$\begin{aligned} LV(e,t) &= e[f(x_N+e,t) - f(x_N,t)] - \sigma e^2 + \frac{1}{2}\widehat{\sigma}^2[g(x_N - z + e) - g(x_N - z)]^2 \\ &\le K_f e^2 - \sigma e^2 + \frac{1}{2}\widehat{\sigma}^2 K_{g+}^2 e^2 \\ &\le (2K_f - 2\sigma + \widehat{\sigma}^2 K_{g+}^2) V(e,t). \end{aligned}$$

Hence, (H2) holds for $c_2 = 2K_f - 2\sigma + \widehat{\sigma}^2 K_{g+}^2$. Second,

$$|V_e B|^2 = |e\widehat{\sigma}[g(x_N - z + e) - g(x_N - z)]|^2 \ge \widehat{\sigma}^2 K_{g-}^2 e^4 = 4\widehat{\sigma}^2 K_{g-}^2 V(e,t)^2$$

so that (H3) holds for $c_3 = 4\widehat{\sigma}^2 K_{g-}^2$. Finally, the condition $c_3 > 2c_2$ requires

$$2\sigma > 2K_f + \widehat{\sigma}^2(K_{g+}^2 - 2K_{g-}^2). \tag{3.4}$$

■

One implication of Theorem 3.1 is that increasing noise intensity can synchronize, in certain conditions, a quorum sensing network. Indeed, when for $K_{g+}^2 < 2K_{g-}^2$, large noise intensities ($\widehat{\sigma}$) can guarantee the fulfillment of (3.2). Here 2σ is nonnegative by definition, and when $K_{g+}^2 < 2K_{g-}^2$, the right-hand side of (3.2) becomes negative for sufficiently high values of $\widehat{\sigma}$. This phenomenon, where noise facilitates synchronization, has been also experimentally observed in many applications [18, 13, 17]. Moreover, the condition given by Theorem 3.1 does not involve the size N, which indicates that node-to-node synchronization will not be affected by the size of the system and can be easily satisfied.

3.2. Node-to-medium synchronization. Assuming the hypotheses of Theorem 3.1 are satisfied as $t \to \infty$, by the definition of node-to-node synchronization, the dynamics of (3.1) converges to the reduced system

$$ds = [f(s,t) + \sigma(z-s)]dt + \widehat{\sigma} g(s-z)dW, \tag{3.5a}$$

$$dz = [h(z,t) - \sigma N(z-s)]dt - \widehat{\sigma} N g(s-z)dW. \tag{3.5b}$$

Note that s and z undergo different intrinsic dynamics for $f \ne h$. We need to discuss the existence of node-to-medium synchronization before studying its stability. Assume there exists a node-to-medium synchronous solution $\hat{s}(t)$. By system (3.5), we know that $\hat{s}(t)$ has to satisfy the following condition:

$$\frac{d\hat{s}}{dt} = f(\hat{s},t) = h(\hat{s},t). \tag{3.6}$$

The trivial case of having the above condition satisfied is to set $f \equiv h$. However, this is not a necessary condition. Consider a constant function $\hat{s}(t) = s^*$ with $f(s^*,t) = h(s^*,t) = 0$. That is, common zeros of the functions f and h are potential candidates for network synchronization. Assuming $\hat{s}$ exists, we give a sufficient condition for node-to-medium synchronization.

Theorem 3.2. *Assume that the hypotheses of Theorem 3.1 are satisfied and that there exists $\hat{s}(t)$ that $f(\hat{s}(t),t) = h(\hat{s}(t),t)$, $\forall t \in \mathbb{R}^+$. Equation (3.1) then achieves node-to-medium synchronization if there exists a constant $K_{fh} \in \mathbb{R}$ such that*

$$(x-y)[f(x,t)-h(y,t)] \leq K_{fh}(x-y)^2$$

and

$$2\sigma(N+1) > 2K_{fh} + \widehat{\sigma}^2(K_{g+}^2 - 2K_{g-}^2)(N+1)^2.$$

Proof. The result can be proven by defining the error as $e(t) = s(t) - z(t)$ and by showing that the trivial solution of this error dynamics is a.s. exponentially stable. Then, from (3.5), we have

$$de = [f(s,t) - h(s+e,t) - \sigma(N+1)e]dt + \widehat{\sigma}(N+1)g(e)dW. \tag{3.7}$$

Now, by hypotheses, we have that $e = 0$ is a solution of (3.7) when $s(t) = \hat{s}(t)$. We study stability of this solution by considering the Lyapunov function $V_e = \frac{1}{2}e^2$ and apply Lemma 2.1 to give

$$LV(e,t) = e[f(e+z,t) - h(z,t) - \sigma(N+1)e] + \frac{1}{2}\widehat{\sigma}^2(N+1)^2 g^2(e) \leq c_2 V_e,$$

where $c_2 = 2K_{fh} - 2\sigma(N+1) + K_{g+}^2\widehat{\sigma}^2(N+1)^2$. Moreover,

$$\Big[e\sigma(N+1)g(e)\Big]^2 \geq c_3 V_e^2,$$

where $c_3 = 4K_{g-}^2\widehat{\sigma}^2(N+1)^2$. Therefore, $e = 0$ is exponentially stable a.s. if $c_3 > 2c_2$, which holds for

$$2\sigma(N+1) > 2K_{fh} + \widehat{\sigma}^2(K_{g+}^2 - 2K_{g-}^2)(N+1)^2. \qquad \blacksquare$$

Note that star networks are a special case of a quorum sensing network when $f = h$ (in this case we have $K_{fh} = K_f$). Comparing the result of Theorem 3.2 for node-to-medium synchronization with Theorem 3.1 for node-to-node synchronization, we see that if $K_{g+}^2 < 2K_{g-}^2$, then node-to-node synchronization guarantees node-to-medium synchronization because

$$2\sigma(N+1) > 2\sigma > 2K_f + \widehat{\sigma}^2(K_{g+}^2 - 2K_{g-}^2) \geq 2K_f + \widehat{\sigma}^2(K_{g+}^2 - 2K_{g-}^2)(N+1)^2.$$

Moreover, in system (2.3) with N nodes and a shared medium, setting $f = h$ implies that the medium z acts like an additional node, undergoing the same intrinsic dynamics as all the other nodes, x_i. Then system (3.1) becomes a special case of network (1.1), where the underlying graph is star-shaped with $N+1$ nodes. By the result in [28], we find that all $(N+1)$ nodes synchronize when

$$\sigma > K_f + \widehat{\sigma}^2(N - N^{-1})K_{g+}^2.$$

Comparing with our result, node-to-node and node-to-medium synchronization is achieved when

$$\sigma > \max\left\{\frac{K_f}{N+1} + \frac{\widehat{\sigma}^2}{2}(N+1)(K_{g+}^2 - 2K_{g-}^2), K_f + \frac{\widehat{\sigma}^2}{2}(K_{g+}^2 - K_{g-}^2)\right\}.$$

Note that both are sufficient conditions for synchronization. In the case where $K_{g+}^2 < 2K_{g-}^2$, our result is less restrictive, while in the case $K_{g-} = 0$, the result from [28] can be less restrictive.

3.3. Application: Multiagent system with common noise. As an explicit illustration of the above analysis, consider the following network, where each individual node dynamics models a decision process [25]. That is, in the model, $f(a,t) = ra - a^3$, and this models an agent that needs to decide among two mutually exclusive opinions [10]:

$$dx_i = [rx_i - x_i^3 + \sigma(z - x_i)]dt + \widehat{\sigma}(x_i - z)dW, \quad i = 1, \dots, N, \tag{3.8a}$$

$$dz = [h(z,t) - \sigma \sum_{j=1}^{N}(z - x_j)]dt - \widehat{\sigma} \sum_{j=1}^{N}(x_j - z)dW, \tag{3.8b}$$

where σ is the agent-station coupling strength and $\widehat{\sigma}$ is the noise level. In this example, we have $f(a,t) = f(a) = ra - a^3$ and $g(a) = a$ from (3.1). Note that the function $f(x) = rx - x^3$ indicates that there are three fixed points of the uncoupled deterministic node dynamics: $x = 0$, which is unstable, and $x = \pm\sqrt{r}$, which are stable. Here $h(z,t)$ describes the intrinsic dynamics of a shared station. If the shared station only acts as an information sharing medium, then $h(z,t) \equiv 0$. Another possibility is that the shared station exhibits the same dynamics as the nodes, which is equivalent to a star network with $N+1$ agents. A third alternative is that the station dynamics can be totally different from the node dynamics. For the system (3.8), we have $K_{g-} = K_{g+} = 1$ and $K_f = r$. Hence, from Theorem 3.1, we know that a sufficient condition for node-to-node synchronization is $2\sigma \geq 2r - \widehat{\sigma}^2$. Once node-to-node synchronization is achieved, (3.8) reduces to the following two-dimensional system:

$$ds = [rs - s^3 + \sigma(z - s)]dt + \widehat{\sigma}(s - z)dW, \tag{3.9a}$$

$$dz = [h(z,t) - \sigma N(z - s)]dt - \widehat{\sigma} N(s - z)dW. \tag{3.9b}$$

In Figure 1, we show an example of noise-induced node-to-node synchronization without node-to-medium synchronization. Note that the candidate for a full node-to-medium synchronization $\hat{s}(t)$ is $\hat{s}(t) = -1, 0, 1$. However, at $t \approx 6$, all nodes synchronized to some function $s(t)$ that is not a constant. This is an example of node-to-node synchronization to some function $s(t)$, which is different than the node-to-medium synchronization function $\hat{s}(t)$. In Figure 2, we present an example of full node-to-medium synchronization.

Both Figures 1 and 2 present time evolution plots of a system for a single initial condition. We can also run a set of initial conditions and track how the resulting cloud of points evolves in time. This is shown in Figures 3 and 4 for $N = 1$ and $N = 20$, respectively, where each dot represents one initial condition. We use the Euler–Maruyama method to simulate the time evolution from each initial condition and track their spatial distribution in the $s - z$ plane. At every time step, each dot is updated with independent noise. Comparing the two figures we see how increasing N results in the system converging to consensus, which is expected from Theorem 3.2. In both plots, we have $f(a) = a - a^3$ and $h(a) = -f(a)$. The reduced system (3.9) thus has three different synchronization states $(\hat{s}, \hat{s})$, where $\hat{s} = -1, 0, 1$. From Figure 4 (f), we see that all initial conditions converge to one of these states. Looking more closely at Figure 4, there appear to be attracting regions at intermediate times, which ultimately converge to the one-dimensional invariant manifold given by $s = z$. In the next section, we explore further how the SDE system (3.9) exhibits characteristics similar to deterministic dynamical systems.

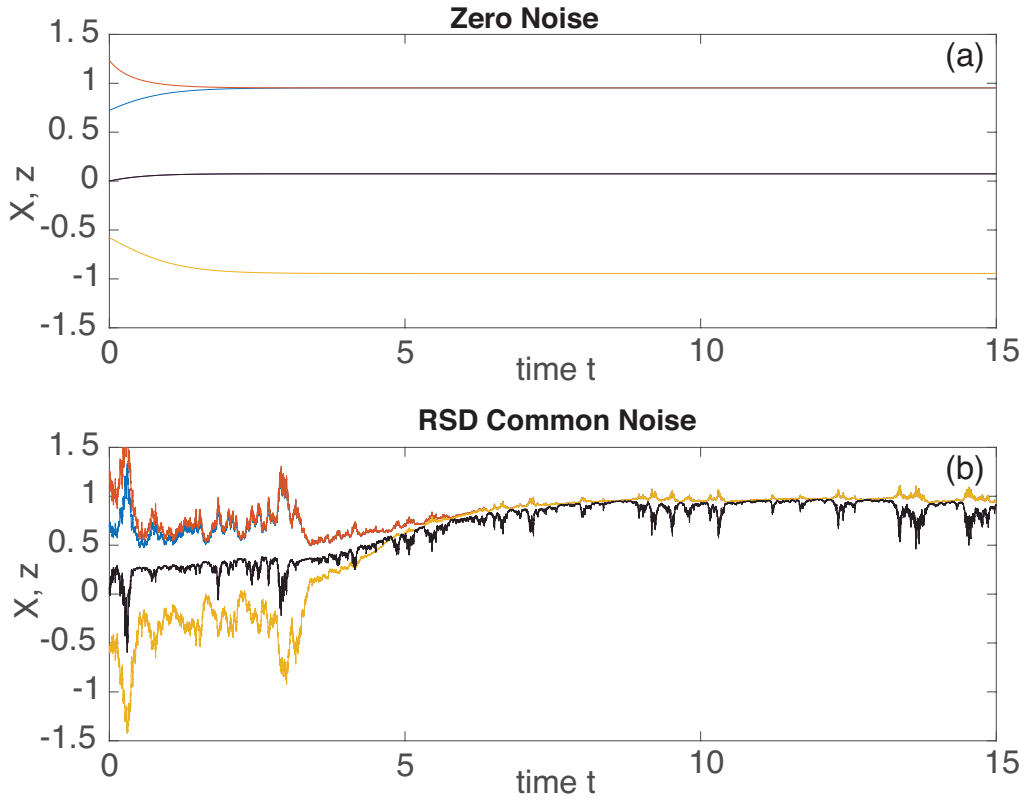

FIGURE 1. *Time evolution of system (3.8) with nodes x_i (colored), $i = 1, \ldots, N$, and the shared medium z (black) for* (a) *zero noise ($\widehat{\sigma} = 0$) and* (b) *nonzero common noise ($\widehat{\sigma} > 0$). In this example, $h(a,t) = h(a) = -2(a - a^3)$ and $N = 3$, $\sigma = 0.1$, $\widehat{\sigma} = 1$, $r = 1$. Here we used the Euler–Maruyama method [11] to simulate the SDE with step size $\delta t = 0.0001$. The initial conditions for x_i are chosen randomly from a standard distribution centered at 0 with standard deviation 1, and $z(0) = 0$. Common noise induces node-to-node synchronization without node-to-medium synchronization.*

3.4. Stochastic invariant manifolds. In this section, we demonstrate the existence of both deterministic and stochastic invariant manifolds (defined below) in the stochastic system (3.9). Similar ideas, which are omitted here for brevity, can be straightforwardly applied to the more general system (3.5). First, we recall the definition of an invariant manifold for a deterministic dynamical system. Consider the differential equation $d\mathbf{x}/dt = f(\mathbf{x})$, $\mathbf{x} \in \mathbb{R}^n$, with flow $\mathbf{x}(t; t_0, \mathbf{x}_0)$ being the solution of the differential equation under the initial condition $\mathbf{x}(t_0) = \mathbf{x}_0$. A set $S \subset \mathbb{R}^n$ is an invariant set for the differential equation if $\forall x_0 \in S$; then $\mathbf{x}(t; t_0, \mathbf{x}_0) \in S$ for all $t \geq t_0$. Moreover, S is called an invariant manifold if S is a manifold.

Example 1. The synchronization manifold $s = z$ for system (3.9) is a deterministic invariant manifold if $h(\cdot) = f(\cdot)$. The proof is fairly straightforward. First, note that the one-dimensional subspace $S_{syn} = \{(s, z) : s = z\} \subset \mathbb{R}^2$ is a manifold. For the initial conditions on the synchronization manifold, that is $(s(0), z(0)) \in S_{syn}$ or equivalently $s(0) = z(0) = s_0 \in \mathbb{R}$. Let $\hat{s}(t)$ denote the unique solution of $\dot{\hat{s}} = f(\hat{s})$ and $\hat{s}(0) = \hat{s}_0$. Then, given $h = f$ and the fact

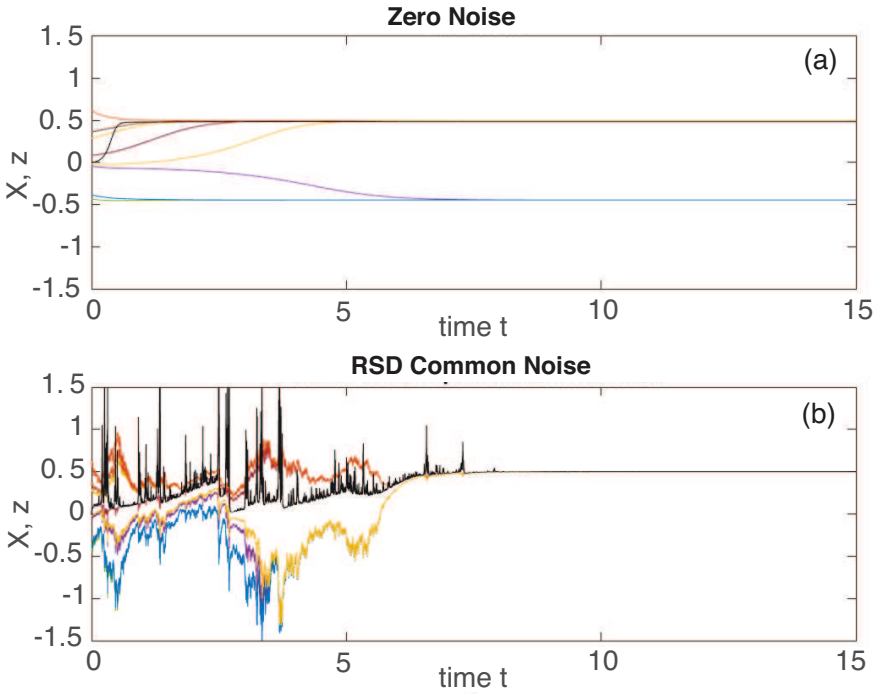

FIGURE 2. *Same as Figure 1 except that* $N = 10$ *and* $h(a) = 10(a - a^3)$. *Common noise now induces both node-to-node and node-to-medium synchronization.*

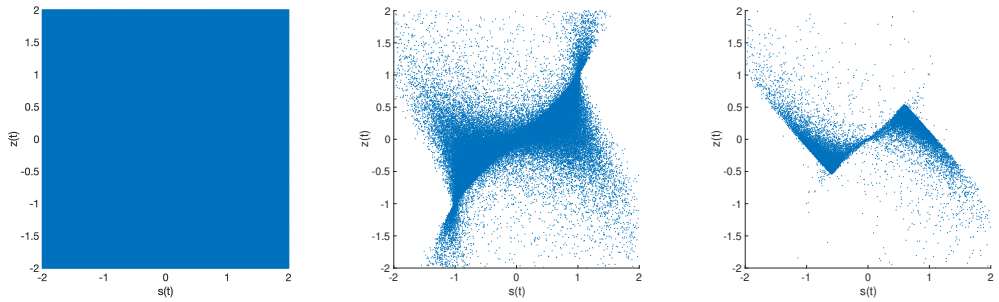

(a) (b) (c)

FIGURE 3. *Time evolution of system* (3.9) *with different initial conditions (blue dots) sampled from a grid* $[-2 : 0.01 : 2] \times [-2 : 0.01 : 2]$; (a) $t = 0$; (b) $t = 1$; (c) $t = 20$. *Here* $h(a) = -(a - a^3) = -f(a)$, $N = 1$, *and all other parameters are the same as Figure 2. It can be seen that node-to-medium synchronization is not achieved.*

that the noise terms vanish on the manifold S_{syn}, we see that if $s(t) = z(t)$ at time t, then

$$ds = f(s(t)) = [s(t) - s(t)^3]dt, \tag{3.10a}$$

$$dz = f(z(t))dt. \tag{3.10b}$$

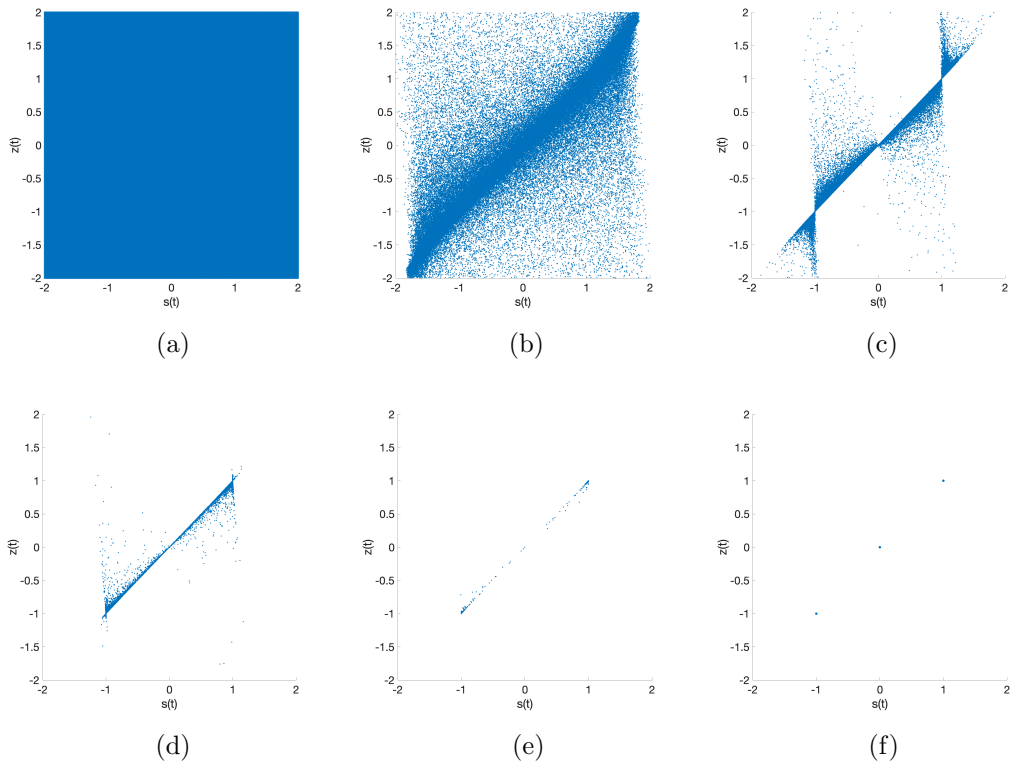

FIGURE 4. *Same as Figure 3 except that $N = 10$: (a) $t = 0$; (b) $t = 0.05$; (c) $t = 1$; (d) $t = 5$; (e) $t = 10$; (f) $t = 20$. In contrast to the previous case, the system converges to one of the three synchronized states, $(1,1), (0,0), (-1,-1)$, as demonstrated in* (f).

Hence, the initial condition (s_0, s_0) yields $s(t) = z(t)$ for all $t \geq 0$, and S_{syn} is a deterministic invariant manifold.

The above example demonstrates how a noise-free manifold can act as an invariant manifold of an SDE. Naturally, with the existence of an invariant manifold, the state space of the full stochastic system is divided into invariant subregions. This motivates us to define a stochastic invariant manifold.

Definition 3. *Consider the autonomous SDE*

$$d\mathbf{x} = F(\mathbf{x})dt + G(\mathbf{x})dW,$$

where $\mathbf{x} \in \mathbb{R}^N$ and $F, G \in \mathcal{C}^2$. A set S is **stochastic invariant** *if for any initial condition $\mathbf{x}(t_0) = \mathbf{x}_0 \in S$ and any realization of the noise process $W(t)$, its solution $\mathbf{x}(t; t_0, \mathbf{x}_0) \in S$ $\forall t \in \mathbb{R}^+$. In addition, such a set S is a* **stochastic invariant manifold** *if S is a manifold.*

In Example 1, we showed that the one-dimensional manifold S_{syn} of the system (3.9) is invariant when $h = f$. It follows that S_{syn} separates $\mathbb{R}^2$ into a pair of two-dimensional stochastic invariant manifolds,

$$D_1 = \{(s,z)|s \geq z\}, \quad D_2 = \{(s,z)|s \leq z\},$$

with $D_1 \cap D_2 = S_{syn}$. This follows from the intermediate value theorem. Without loss of generality, let $\mathbf{x}_0 \in D_1 \backslash S_{syn}$, and assume there exists a time $t_1 > t_0$, where $\mathbf{x}(t_1; t_0, \mathbf{x}_0) \in D_2 \backslash S_{syn}$. Since the given SDE has the integral form

$$\mathbf{x}(t) = \mathbf{x}_0 + \int_{t_0}^{t} \mathbf{F}(x(s))ds + \int_{t_0}^{t} \mathbf{G}(x(s))d\mathbf{W}(s)$$

and $\mathbf{F}, \mathbf{G}$, and $\mathbf{W}(s)$ are all continuous, we know that $\mathbf{x}(t)$ is continuous. This implies that there exists a time t^*, where $\mathbf{x}(t^*) \in S_{syn}$. By the definition of a deterministic invariant manifold, we know that $\mathbf{x}(t) \in S_{syn}, \forall t > t^*$, which contradicts $\mathbf{x}(t_1) \in D_2 \backslash S_{syn}$, where $t_1 > t^*$.

The existence of stochastic invariant manifolds provides some information about how stochastic trajectories depend on initial conditions, i.e., whether the initial conditions are in D_1 or D_2. However, it does not answer the question of what is the basin of attraction for different consensus states, which in our example are $(-1, -1)$, $(0, 0)$, and $(1, 1)$. In order to address this question, we show in the next example that for a particular choice of h, there exists another one-dimensional invariant manifold that is transversal to the synchronization manifold S_{syn}.

Example 2. Let $h(a) = -Nf(-a/N)$ for system (3.9). In contrast to Example 1, there is now only one candidate node-to-medium synchronization state when $N > 1$, namely, $(0, 0)$. Set $C = Ns + z$, where different C values represent different level curves. Multiplying (3.9a) by N and adding to (3.9b) yields the deterministic equation

$$dC = d(Ns + z) = [Nf(s) + h(z)]dt \tag{3.11}$$

or

$$\frac{dC}{dt} = [Nf(s) + h(z)], \tag{3.12}$$

which describes how the dynamics between different level curves are defined. In particular, when $C = 0$, we have $Ns + z = 0$, or $s = -z/N$. Since for our choice of h, $h(a) = -f(a/N)$, for any point (s, z) on the manifold

$$M = \{C = 0\} = \{(s, z) | Ns + z = 0\},$$

it follows that $Nf(s) + h(z) = Nf(s) + h(-Ns) = Nf(s) - Nf(s) = 0$. Therefore, M is a stochastic one-dimensional invariant manifold. (Although the dynamics is constrained to remain on M, it is still stochastic.) Using similar arguments to the analysis of Example 1, we know that the invariant manifold M separates $\mathbb{R}^2$ into a pair of two-dimensional stochastic invariant manifolds,

$$\widehat{D}_1 = \{(s, z) | s \geq -z/N\}, \quad \widehat{D}_2 = \{(s, z) | s \leq -z/N\},$$

with $\widehat{D}_1 \cap \widehat{D}_2 = M$. Moreover, by (3.12), the sign of $Nf(s) + h(z)$ determines whether C is increasing or decreasing. Thus, yet another way to partition the phase plane is in terms of the one-dimensional manifold

$$\widehat{M} = \{\dot{C} = 0\} = \{(s, z) | Nf(s) + h(z) = 0\}.$$

Although $M \subset \widehat{M}$, the total space $\widehat{M}$ is not invariant. One can think of $\widehat{M}$ as the nullcline for the variable C.

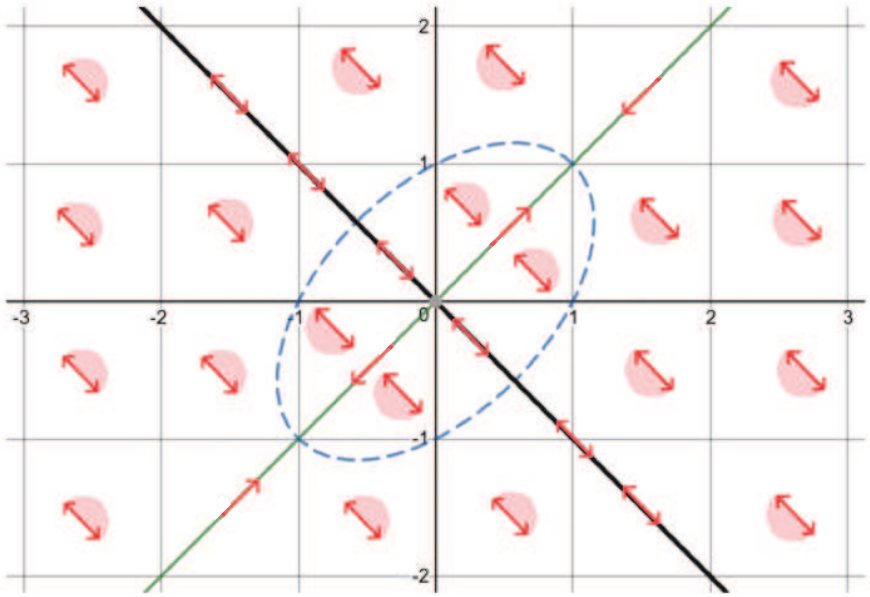

FIGURE 5. *Phase plane diagram for the SDE system (3.9) with $h(a) = f(a) = a - a^3$ and $N = 1$. The thick black line represents the invariant manifold M, and the green line represents the invariant manifold S_{syn}. The red arrows represent the possible directions along these manifolds. The two one-dimensional manifolds divide the phase plane into four two-dimensional stochastic invariant manifolds. The manifold $\widehat{M}$ is given by the union of M and the closed dotted curve. The sign of $f(s)+h(z)$ determines whether $C = s+z$ is increasing or decreasing, as indicated by the shaded regions.*

Example 3. In the special case of $N = 1$, conditions $h(a) = f(a)$ and $h(a) = -Nf(-\frac{a}{N})$ are equivalent. Having both conditions satisfied ($N = 1$ and $h = f$) results in an SDE system with two different invariant manifolds. We can then construct a stochastic phase plane diagram, as shown in Figure 5. One major consequence of the existence of a stochastic invariant manifold is that any initial condition in $\widehat{D}_1$ (top right) cannot cross the manifold M to approach the point $(-1,-1)$, and any initial condition in $\widehat{D}_2$ (bottom left) cannot cross M to approach the point $(1,1)$. Moreover, the point $(0,0)$ is not stochastically stable a.s. since it is an unstable equilibrium of the noise-free synchronization manifold S_{sync}. Therefore, the basin of attraction of the consensus state $(1,1)$ is $\widehat{D}_1$, and the basin of attraction of the consensus state $(-1,-1)$ is $\widehat{D}_2$, whereas $(0,0)$ effectively acts as a stochastic saddle node. This is verified by the numerical simulations shown in Figures 6 and 7. In Figure 6, we colored the different initial conditions based on the sign of $C(0) = s(0) + z(0)$, where the yellow dots represent initial conditions started from $\widehat{D}_1 = \{(s,z)|s \geq -z\}$ and the blue dots represent initial started from $\widehat{D}_2 = \{(s,z)|s \leq -z\}$. Figure 6 shows the path of convergence for different initial conditions, and from the plot we see that almost all initial conditions eventually converge to $(1,1)$ or $(-1,-1)$. Figure 7 shows in detail the basins of attraction. Here the invariant manifold M serves as a seperatrix such that initial conditions in $\widehat{D}_1$ (yellow) converge to $(1,1)$, whereas initial conditions in $\widehat{D}_2$ (blue) converge to $(-1,-1)$; the subset of initial conditions located on the stochastic invariant manifold M converge to $(0,0)$. (Note that the stochastic invariant manifold $C = 0$ in Example 2 does not act as a stochastic

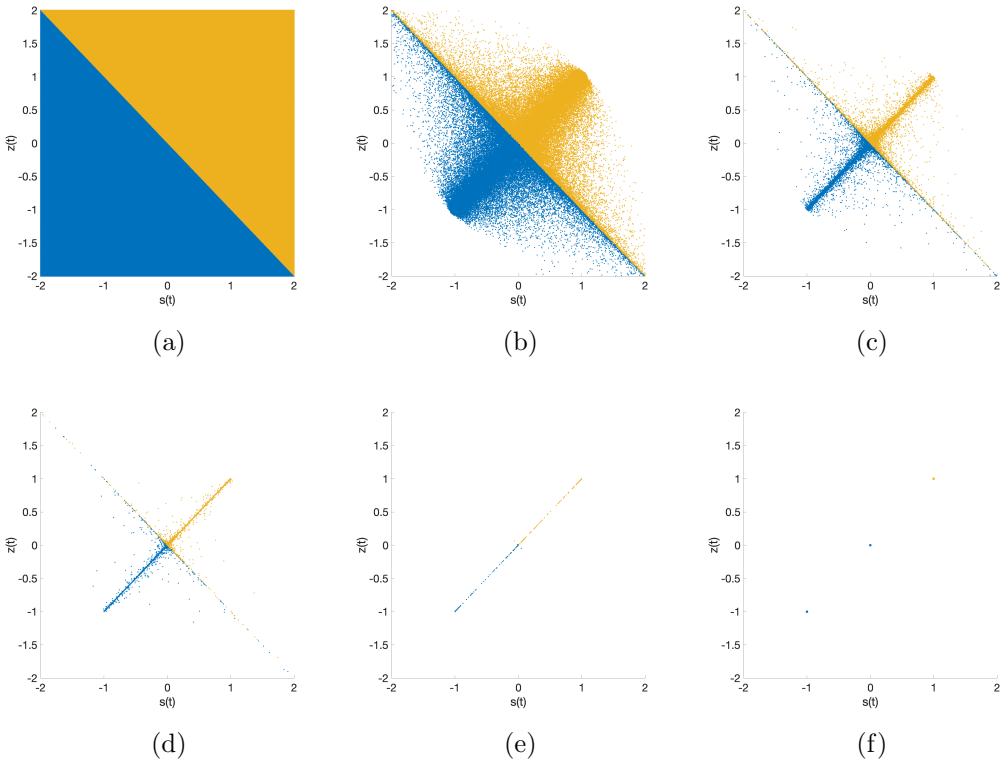

FIGURE 6. *Time evolution of system* (3.9)*, where* $f(a,t) = h(a,t) = a - a^3$*,* $g(a,t) = a$*,* $N = 1$*,* $\sigma = 0.1, \widehat{\sigma} = 1, dt = 0.0001$*, with different initial conditions (blue dots) sampled from grid* $[-2 : 0.01 : 2] \times [-2 : 0.01 : 2]$*:* (a) $t = 0$*;* (b) $t = 1$*;* (c) $t = 5$*;* (d) $t = 10$*;* $t = 30$*;* $t = 60$*. In this example,* $(0,0)$ *is a stochastic saddle point.*

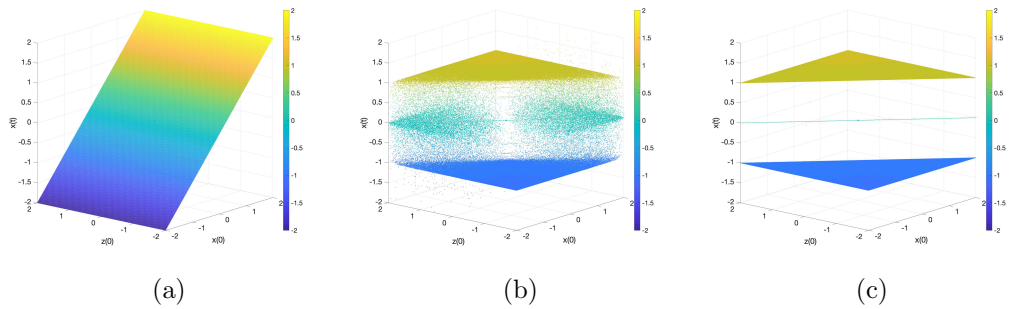

FIGURE 7. *Three-dimensional plot for Figure* 6*, where the* x, y*-axes represent the coordinates of the initial conditions and the* z*-axis represent* $x(t)$ *at* (a) $t = 0$*;* (b) $t = 2$*;* (c) $t = 40$*.*

separatrix for $N > 1$ because the two states $(1,1)$ and $(-1,-1)$ are no longer node-to-medium synchronization states.)

3.5. Increasing the number of nodes. Even when the SDE system does not support any one-dimensional invariant manifolds, we can still use phase plane analysis in order to understand particular features of the paths of convergence to synchronized states. Let's revisit

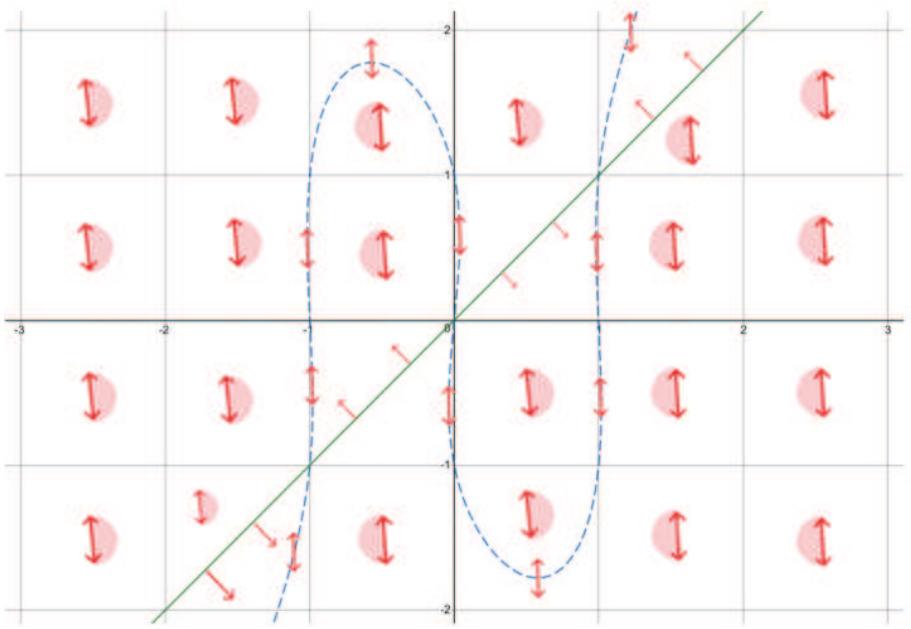

FIGURE 8. *Phase plane diagram for the SDE system studied in Figure 4. The green line represents the synchronization manifold S_{syn} and the blue dotted line represents the level curve $Nf(s)+h(z)=0$, for which $d(Ns+z)/dt=0$. The red arrows represent the possible directions along these manifolds and are almost vertical for large N.*

our model system (3.9) with $h(a)=-f(a)$. When the number of nodes is large, the system will be dominated by the N-dependent terms. In particular, z will be a fast variable, where

$$dz \approx -\sigma N(z-s)dt - \widehat{\sigma} N(s-z)dW.$$

Using a similar stability analysis to section 3, one can show that the synchronized state $z=s$ is a.s. exponentially stable. This implies that the fast variable z will quickly drive the trajectory to a neighborhood of the synchronization manifold S_{syn}, ultimately resulting in synchronization, as seen in Figure 4. Moreover, by plotting the level curve $C=0$ in the phase plane, as seen in Figure 8, we see that trajectories tend to approach this level curve before ultimately converging to the synchronized states, which helps explain why we observe sharp convergence to trapping-like regions around time $t=1$ in Figure 4(c).

4. Network synchronization under independent noise. We now turn to the case where the noise associated with each node-to-medium link is independent rather than common to all of the nodes. The corresponding stochastic differential equation is

$$dx_i = [f(x_i,t)+\sigma(z-x_i)]dt + \widehat{\sigma} g(x_i-z)dW_i, \quad i=1,\dots,N, \tag{4.1a}$$

$$dz = \left[h(z,t) - \sigma\sum_{j=1}^{N}(z-x_j)\right]dt - \widehat{\sigma}\sum_{j=1}^{N} g(x_j-z)dW_j, \tag{4.1b}$$

where the $W_i(t)$ are independent Wiener processes. It is straightforward to see that with independent noise, node-to-node synchronization is not possible without node-to-medium synchronization. Therefore, we directly present the proof of node-to-medium synchronization.

Theorem 4.1. *Consider the system* (4.1)*, and let Assumptions* 1 *and* 2 *hold. Then the network achieves node-to-medium synchronization if*

$$(x-y)[f(t,x)-h(t,y)] \le K_{fh}(x-y)^2$$

and

$$2\sigma > 2K_{fh} + \widehat{\sigma}^2\left[(N+1)K_{g+}^2 - 2\frac{1}{N}K_{g-}^2\right].$$

Proof. Following along similar lines to the previous proofs, we introduce the error dynamics as $\mathbf{e} = [e_1, \dots, e_N]^T$, where $e_i = x_i - z$ for $i = 1, \dots, N$ and

$$de_i = \left[f(t,x_i) - h(t,z) - \sigma e_i - \sigma\sum_{j=1}^{N} e_j\right]dt + \widehat{\sigma}\left[g(e_i)db_i + \sum_{j=1}^{N} g(e_j)dW_j\right]. \tag{4.2}$$

Equivalently, we have

$$d\mathbf{e} = A(X)dt + B(\mathbf{e})dW,$$

where $A = \mathbf{F} - \mathbf{H} - \sigma L\mathbf{e}$, $\mathbf{F} = [f(t,x_1), \dots, f(t,x_N)]^T$, $\mathbf{H} = [h(t,z), \dots, h(t,z)]^T$ with

$$L = \begin{bmatrix} 2 & 1 & \dots & 1 \\ 1 & 2 & \dots & 1 \\ 1 & 1 & \dots & 2 \end{bmatrix}$$

and $B = \widehat{\sigma}L\mathbf{G}$, $\mathbf{G} = \mathrm{diag}\{g(t,e_1), \dots, g(t,e_N)\}$, $dW = [dW_1, \dots, dW_N]^T$. Similarly, $\mathbf{e} = 0$ is a solution only when there exists function $s(t)$, where $x_i(t) = z(t) = s(t)$ such that $f(t,s) = h(t,s)$ $\forall t \in \mathbb{R}^+$. Pick the Lyapunov function to be $V(\mathbf{e}) = \mathbf{e}^T\mathbf{e}/2$. Following Lemma 2.1, we next find bounds for $LV(\mathbf{e})$ and $|V_{\mathbf{e}}B|^2$.

(H2) $V_{\mathbf{e}}A = \sum_j e_j[f(t,z+e_j) - h(t,z)] - \sigma\mathbf{e}^T L\mathbf{e}$. By some calculation, we know that matrix L has eigenvalues $\lambda = 1, \dots, 1, N+1$. Since L is a symmetric real matrix, we get $\mathbf{e}^T L\mathbf{e} \in [\lambda_{min}\mathbf{e}^T\mathbf{e}, \lambda_{max}\mathbf{e}^T\mathbf{e}] = [\mathbf{e}^T\mathbf{e}, (N+1)\mathbf{e}^T\mathbf{e}]$. Therefore, $V_{\mathbf{e}}A \le 2(K_{fh} - \sigma)V(\mathbf{e})$.

Next, by algebraic calculation and Assumption 2, we get

$$\frac{1}{2}tr\{B^T V_{\mathbf{ee}} B\} = \widehat{\sigma}^2\frac{N+1}{2}\sum_{j=1}^{N} g^2(e_j) \le \widehat{\sigma}^2\frac{N+1}{2}K_{g+}^2\mathbf{e}^T\mathbf{e}.$$

Then we have

$$LV = V_{\mathbf{e}}A + \frac{1}{2}tr\{B^T V_{\mathbf{ee}} B\} \le c_2 V(t,e),$$

where $c_2 = 2K_{fh} - 2\sigma + (N+1)\widehat{\sigma}^2 K_{g+}^2$, and

(H3) $|V_eB|^2 = \widehat{\sigma}^2|\mathbf{e}^T L\mathbf{G}|^2 \geq 0$, where

$$|\mathbf{e}^T L\mathbf{G}|^2 = \sum g_j^2[(\Sigma e_k) + e_j)]^2 \geq K_{g-}^2 \sum e_j^2[(\Sigma e_k) + e_j]^2 \geq \frac{1}{N} K_{g-}^2 |\mathbf{e}^T\mathbf{e}|^2.$$

Therefore,

$$|V_eB|^2 \leq c_3 V^2(t, e)$$

with $c_3 = 4\widehat{\sigma}^2 \frac{1}{N} K_{g-}^2$ Put everything together, we get that the synchronization state is exponentially stable a.s. when $c_3 > 2C_2$, that is, when

$$2\widehat{\sigma}^2 \frac{1}{N} K_{g-}^2 > 2K_{fh} + (N+1)\widehat{\sigma}^2 K_{g+}^2 - 2\sigma$$

or

$$2\sigma > 2K_{fh} + \widehat{\sigma}^2 \left[(N+1)K_{g+}^2 - 2\frac{1}{N} K_{g-}^2 \right].$$

Note that this result is broader than the one found in [29] because in that paper $c_3 = 0$, which eliminated the case of independent noise-derived synchronization.

Example 4. We illustrate the above result for the system (3.8) with independent noise, that is,

$$dx_i = [rx_i - x_i^3 + \sigma(z - x_i)]dt + \widehat{\sigma}(x_i - z)db_i, \quad i = 1, \ldots, N, \tag{4.3a}$$

$$dz = \left[h(t, z) - \sigma \sum_{j=1}^{N} (z - x_j) \right] dt - \widehat{\sigma} \sum_{j=1}^{N} (x_j - z)db_j. \tag{4.3b}$$

Using the same initial condition and parameters as Figure 2 we obtain the plots shown in Figure 9. Note that we can apply a similar stochastic invariant manifold analysis to the independent noise case, which we have omitted here for brevity.

5. Discussion. In this paper, we analyzed two synchronization phenomena (node-to-node and node-to-medium synchronization) in quorum sensing networks, where nodes communicate indirectly via a shared environmental variable (or medium) and where the communication links are noisy. The noise diffusion processes considered in the paper were state dependent (RSD noise diffusion processes). Also, the medium was characterized by its own intrinsic dynamics, and this was, in general, different from the internal dynamics of the nodes. In this context, we showed that, in case of common noise, the network can achieve both node-to-node synchronization, i.e., a state where nodes are all synchronized with each other, and node-to-medium synchronization, i.e., a state where the nodes are not only synchronized with each other but also synchronized with the medium. On the other hand, in the case of independent noise, node-to-medium synchronization is necessary for node-to-node synchronization. In order to further characterize the onset of synchronization in these quorum sensing networks, we also carried out a stochastic phase plane analysis of their dynamics on the synchronization manifold. In particular, we constructed examples of one-dimensional stochastic invariant manifolds and nullclines, which played a crucial role in organizing the flow of trajectories toward node-to-medium synchronized states.

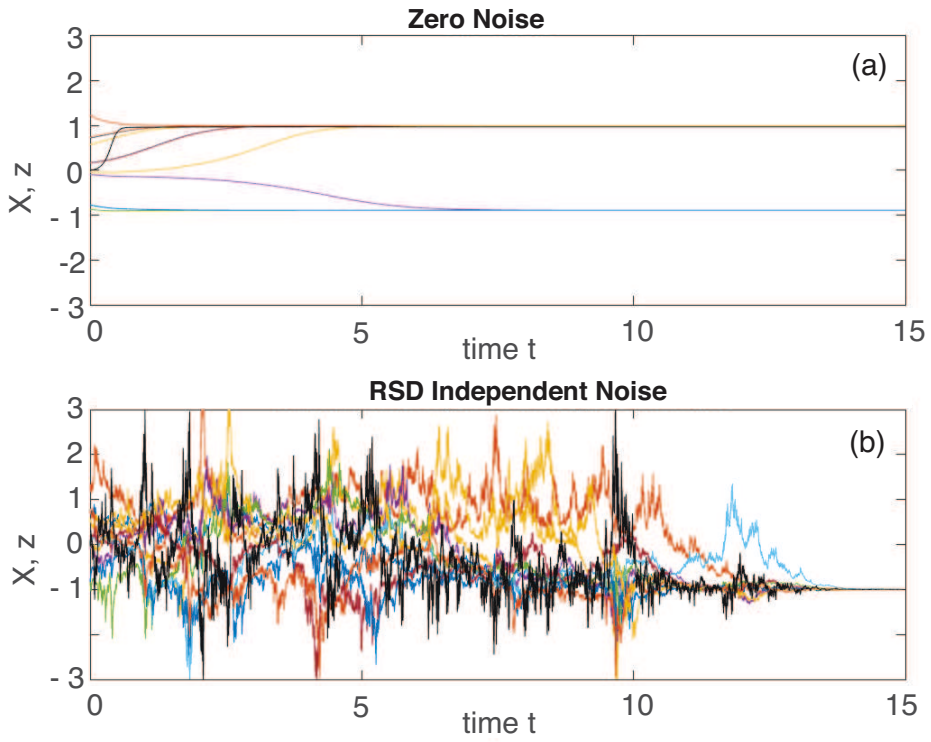

FIGURE 9. *Time evolution of system (4.3) with nodes x_i(colored), $i = 1, \ldots, N$, and the shared medium z(black) for* (a) *zero noise ($\widehat{\sigma} = 0$) and* (b) *nonzero independent noise ($\widehat{\sigma} > 0$). It can be seen that independent noise induces synchronization. All parameters and initial conditions are the same as Figure 2.*

A necessary condition for node-to-medium synchronization is that the internal node dynamics $f(x,t)$ and internal medium dynamics $h(z,t)$ have the same zeros. In the case of bacterial quorum sensing networks, cells are coupled with the extracelluar environment by the diffusive exchange of autoinducers. In this case, the medium z is the signal concentration in the extracelluar environment, and the node x_i is the intracellular signal concentration in cell i. In [2], the internal medium dynamics $h(z,t) = -\gamma z$ represents the decay of the extracellular autoinducer z with decay rate γ. Here $h(z,t) = 0$ only when $z = 0$. However, the internal node dynamics $f(x,t)$ is determined by the in-cell chemical reactions and $f(0,t) \neq 0$. Therefore, in this case, f and h have different zeros, so, by the results of our paper, node-to-medium synchronization cannot be achieved. Consequently, $x_i(t)$ and $z(t)$ will still be affected by noise even when node-to-node synchronization is achieved. Intuitively speaking, it may be useful for bacterial quorum sensing systems to be sensitive to different levels of environmental noise. This is also related to the so-called *diffusion sensing* hypothesis, whereby multipathway quorum sensing allows bacteria to react not only to cell density but also to the mass-transfer rate of the extracellular environment [8]. Our future research will involve extending the results of this paper to consider more general (nonlinear) node-to-medium coupling terms and intrinsic noise arising from the nodes' internal dynamics.

REFERENCES

[1] D. Bauso, H. Tembine, and T. Baar, *Opinion dynamics in social networks through mean-field games*, SIAM J. Control Optim., 54 (2016), pp. 3225–3257.

[2] P. C. Bressloff, *Ultrasensitivity and noise amplification in a model of V. harveyi quorum sensing*, Phys. Rev. E, 93 (2016), 062418.

[3] R. Caginalp and B. Doiron, *Decision dynamics in groups with interacting members*, SIAM J. Appl. Dyn. Syst., 16 (2017), pp. 1543–1562.

[4] S. P. Cornelius, W. L. Kath, and A. E. Motter, *Realistic control of network dynamics*, Nat. Commun., 4 (2013), 1942.

[5] P. deLellis, M. di Bernardo, and G. Russo, *On QUAD, Lipschitz and contracting vector fields for consensus and synchronization of networks*, IEEE Trans. Circuits Syst. I, 58 (2011), pp. 576–583.

[6] P. DeLellis, M. di Bernardo, T. E. Gorochowski, and G. Russo, *Synchronization and control of complex networks via contraction, adaptation and evolution*, IEEE Circuits Syst. Mag., 10 (2010), pp. 64–82.

[7] A. Eldar and M. B. Elowitz, *Functional roles for noise in genetic circuits*, Nature, 467 (2010), pp. 167–173.

[8] G. Fan and P. C. Bressloff, *Population model of quorum sensing with multiple parallel pathways*, Bull. Math. Biol., 79 (2017), pp. 2599–2626.

[9] J. Garcia-Ojalvo, M. B. Elowitz, and S. H. Strogatz, *Modeling a synthetic multicellular clock: Repressilators coupled by quorum sensing*, Proc. Natl. Acad. Sci., 101 (2004), pp. 10955–10960.

[10] R. Grasman, H. van der Maas, and E. Wagenmakers, *Fitting the cusp catastrophe in R: A cusp-package primer*, J. Stat. Softw., 32 (2009), pp. 1–28.

[11] D. J. Higham, *Stochastic ordinary differential equations in applied and computational mathematics*, IMA J. Appl. Math., 76 (2011), pp. 449–474.

[12] D. Hong, W. M. Sidel, S. Man, and J. V. Martin, *Extracellular noise-induced stochastic synchronization in heterogeneous quorum sensing network*, J. Theoret. Biol., 245 (2007), pp. 726–736.

[13] C. H. Ko, Y. R. Yamada, D. K. Welsh, E. D. Buhr, A. C. Liu, E. E. Zhang, M. R. Ralph, S. A. Kay, D. B. Forger, and J. S. Takahashi, *Emergence of noise-induced oscillations in the central circadian pacemaker*, PLoS Biol., 8 (2010), e1000513.

[14] A. Kraskov, R. Q. Quiroga, L. Reddy, I. Fried, and C. Koch, *Local field potentials and spikes in the human medial temporal lobe are selective to image category*, J. Cogn. Neurosci., 19 (2007), pp. 479–492.

[15] T. Li, F. Wu, Fuke, and J.-F. Zhang, *Multi-agent consensus with relative-state-dependent measurement noises*, IEEE Trans. Automat. Control, 59 (2014) pp. 2463–2468

[16] X. Mao, *Stochastic Differential Equations and Applications*, Woodhead Publishing, Cambridge, 1997.

[17] M. D. McDonnell and L. M. Ward, *The benefits of noise in neural systems: Bridging theory and experiment*, Nat. Rev. Neurosci., 12 (2011), 415.

[18] J. H. Meng and H. Riecke, *Synchronization by uncorrelated noise: Interacting rhythms in interconnected oscillator networks*, Sci. Rep., 8 (2018), 6949.

[19] M. B. Miller and B. Bassler, *Quorum sensing in bacteria*, Annu. Rev. Microbiol., 55 (2001), pp. 165–199.

[20] C. D. Nadell, J. B. Xavier, S. A. Levin, and K. R. Foster, *The evolution of quorum sensing in bacteria biofilms*, PLoS Comput. Biol., 6 (2008), p. e14.

[21] M. Newman, *The structure and function of complex networks*, SIAM Rev., 45 (2003), pp. 167–256.

[22] W. L. Ng and B. Bassler, *Bacterial suorum-sensing network architectures*, Annu. Rev. Genet., 43 (2009), pp. 197–222.

[23] B. Oksendal, *Stochastic Differential Equations: An Introduction with Applications (Universitext)*, 6th ed., Springer, New York, 2007.

[24] K. Papenfort and B. L. Bassler, *Quorum sensing signal–response systems in Gram-negative bacteria*, Nat. Rev. Microbiol., 14 (2016), pp. 576–588.

[25] T. Potston and I. Stewart, *Catastrophe Theory and its Applications*, Dover, 1997.

[26] M. Rotoli, G. Russo, and M. di Bernardo, *Stabilizing quorum-sensing networks via noise*, IEEE Trans. Circuits Syst. II: Express Briefs, 65 (2018), pp. 647–651.

[27] G. Russo and R. Shorten, *On common noise-induced synchronization in complex networks with state-dependent noise diffusion processes*, Phys. D, 369 (2018), pp. 47–54.
[28] G. Russo and J. J. E. Slotine, *Global convergence of quorum-sensing networks*, Phys. Rev. E, 82 (2010), 041919.
[29] G. Russo, F. Wirth, and R. Shorten, *On synchronization in continuous-time networks of nonlinear nodes with state-dependent and degenerate noise diffusion*, IEEE Trans. Automat. Control, 64 (2019), pp. 389–395.
[30] J. Touboul, G. Hermann, and O. Faugeras, *Noise-induced behaviors in neural mean field dynamics*, SIAM J. Appl. Dyn. Syst., 11 (2012), pp. 49–81.
[31] J. Wang and N. Elia, *Distributed averaging under constraints on information exchange: Emergence of levy flights*, IEEE Trans. Automat. Control, 57 (2012), pp. 2435–2449.
[32] D. Xue, S. Hirche, and M. Cao, *Opinion behavior analysis in social networks under the influence of coopetitive media*, IEEE Trans. Network Sci. Eng., (2019), pp. 1–13.
[33] L. Zino, A. Rizzo, and M. Porfiri, *Modeling memory effects in activity-driven networks*, SIAM J. Appl. Dyn. Syst., 17 (2018), pp. 2830–2854.